

Lipid based drug delivery systems: Kinetics by SANS

D Uhríková¹, J Teixeira², L Hubčík¹, A Búcsi¹, T Kondela¹, T Murugova³ and O I Ivankov³

¹Faculty of Pharmacy, Comenius University in Bratislava, Odbojárov 10, 832 32 Bratislava, Slovakia

²Laboratoire Léon Brillouin (CEA/CNRS), CEA Saclay, 91191 Gif-sur-Yvette Cedex, France

³Frank Laboratory of Neutron Physics, JINR, Joliot-Curie 6, 141980 Dubna, Moscow region, Russia

uhrikova@fpharm.uniba.sk

Abstract. N,N-dimethyldodecylamine-N-oxide ($C_{12}NO$) is a surfactant that may exist either in a neutral or protonated form depending on the pH of aqueous solutions. Using small angle X-ray diffraction (SAXD) we demonstrate structural responsivity of $C_{12}NO$ /dioleoylphosphatidylethanolamine (DOPE)/DNA complexes designed as pH sensitive gene delivery vectors. Small angle neutron scattering (SANS) was employed to follow kinetics of $C_{12}NO$ protonization and DNA binding into $C_{12}NO$ /DOPE/DNA complexes in solution of 150 mM NaCl at acidic condition. SANS data analyzed using paracrystal lamellar model show the formation of complexes with stacking up to ~32 bilayers, spacing ~ 62 Å, and lipid bilayer thickness ~37 Å in 3 minutes after changing pH from 7 to 4. Subsequent structural reorganization of the complexes was observed along 90 minutes of SANS measurements.

1. Introduction

Since almost thirty years are complexes of DNA with cationic liposomes studied as potential non-viral vectors for gene therapy [1, 2]. Relationship between the structure of gene delivery vectors and their transfection efficiency have been studied widely, although conclusions are not all consistent. Significant efforts converged in the past years towards the design and development of on-demand delivery systems.

We focus our attention on pH responsive lipid based DNA delivery systems (lipoplexes). Cellular components such as cytoplasm, endosomes, lysosomes, endoplasmic reticulum, etc. are known to keep their own characteristic pH values. For example, the pathway of the gene-vector complex is accompanied by the drop in pH from physiological (pH 7.4) to acidic in lysosome (pH 4.5). Hence, pH-responsive carriers are aimed at increasing the intracellular drug bioavailability by rapidly releasing their payload in the endosomes after cellular uptake [3], and/or facilitating the drug transit to the cytoplasm [4]. pH responsive liposomes are, generally, constructed as a mixture of dioleoylphosphatidylethanolamine (DOPE) and titrable amphiphiles [3, 5, 6]. It is postulated that effective pH responsive formulations should be able to change a property in a narrow pH window.

N,N-dimethyldodecylamine-N-oxide ($C_{12}NO$) (Figure 1) is a surfactant that may exist either in neutral or cationic protonated form depending on the pH of aqueous solutions. A strong polar N – O



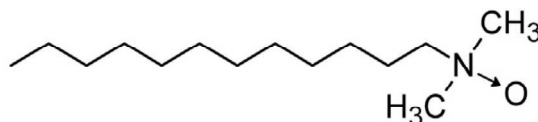


Figure 1. Structure of N,N-dimethyldodecylamine-N-oxide ($C_{12}NO$)

bond with a high electron density on oxygen yields the protonation of molecules $C_{12}N^+OH$ at acidic pH ($pK \sim 5$) [7, 8]. $C_{12}NO$ is widely used in pharmaceutical and cosmetic formulations, as detergent in household dish washing liquids and surface cleaners and in various areas of industry [9, 10]. An amphiphile $C_{12}NO$ incorporates into the biological membrane and can induce changes of fluidity [11], and thickness [12–15] of lipid bilayers. At high concentration $C_{12}NO$ destabilizes lipid bilayers forming non-lamellar phases or mixed micelles [16]. N,N-dimethylalkylamine-N-oxides display antimicrobial [17], immunomodulatory [18] or antiphotosynthetic activity [11]. However, their toxicity is reported as low-to moderate level [9, 19]. Interacting with DNA, $C_{12}NO$ induces a coil – globule phase transition responsive to changes in pH as documented by fluorescence microscopy [20]. The strong influence of pH on DNA/ $C_{12}NO$ interaction was confirmed also by others experimental methods including turbidimetry and dynamic light scattering [21], dielectric spectroscopy and circular dichroism [22], fluorescence with pH sensitive probe [23], and viscosity measurements [24].

Our small angle X-ray diffraction (SAXD) experiments revealed the rich structural polymorphism of lipoplexes due to DNA interaction with $C_{12}NO$ /DOPE vesicles [25]. In neutral solutions, the DNA uptake is low, and a lamellar L_α phase formed by $C_{12}NO$ /DOPE prevails in the complexes at $0.2 \leq C_{12}NO/DOPE \leq 0.6$ mol/mol. In acidic conditions, a condensed inverted hexagonal phase H_{II}^C is observed at $C_{12}NO/DOPE = 0.2$ mol/mol. Higher content of $C_{12}NO$ induces hexagonal to lamellar phase transition. Both phases L_α^C and H_{II}^C coexist in complexes for compositions $0.3 \leq C_{12}NO/DOPE \leq 0.4$ mol/mol and $pH = 4.9–6.4$. Their commensurate lattice parameters, $a_H^C \approx d_L^C$, suggest that L_α^C and H_{II}^C phases are epitaxially related. Instead, at the same composition but $pH \sim 7$, the mixture forms a cubic phase ($Pn3m$) when the complexes are heated to $80^\circ C$ and cooled down to $20^\circ C$. A large portion of the surfactant ($C_{12}NO/DOPE > 0.5$) stabilizes the L_α^C phase in $C_{12}NO$ /DOPE/DNA complexes and the distance between DNA strands (d_{DNA}) is modulated by the pH value. Both composition and pH affect the DNA binding in the complexes reaching up to $\sim 95\%$ of the DNA total amount at acidic conditions.

Consequently, $C_{12}NO$ shows low toxicity and good pH responsivity in both aspects: DNA binding and structural polymorphism of the complexes. In the present study we focus our attention on kinetics of $C_{12}NO$ responsivity to changes of pH, i.e. the protonation of the surfactant molecules and DNA binding. Following our knowledge about polymorphic behavior of the system [25], we have chosen vesicles with a composition $C_{12}NO/DOPE=1$ mol/mol, at which a lamellar phase was the only detected structure. SAXD and SANS were used. SANS experiments were performed with the aim to follow structural changes of the vesicles due to DNA binding in the process of $C_{12}NO$ protonation, profiting of the scattering contrast between protonated system in a deuterated solvent. SAXD shows structural changes in complexes as a function of pH of solutions.

2. Material and Methods

2.1. Sample preparation

Neutral phospholipid DOPE (1,2-dioleoyl-sn-glycero-3-phosphoethanolamine) was purchased from Avanti Polar Lipids, Inc., USA. Deuterium oxide (D_2O , 99.9 %), N,N-dimethyldodecylamine-N-oxide ($C_{12}NO$) and highly polymerized DNA (sodium salt) type XIV from herring testes (average M_r of nucleotide = 308) were purchased from Sigma-Aldrich, USA. NaCl was obtained from Lachema, Brno, Czech Republic. The chemicals were of the analytical grade and were used without further purification. The aqueous solutions were prepared either with redistilled water or D_2O . 150 mM NaCl

was used as buffer. The solution of DNA was prepared by dissolving in a 150 mM NaCl solution. The precise value of DNA concentration was determined by spectrophotometer [25].

DOPE and $C_{12}NO$ were dissolved in chloroform and mixed to molar ratio $C_{12}NO/DOPE=1$. Lipid mixture was dried under a stream of gaseous nitrogen and the residue of chloroform was removed under vacuum. For SAXD experiment, the dry mixture was hydrated by the solution of DNA and the final volume of samples was adjusted by 150 mM NaCl to 2 ml. The pH of samples was adjusted by stepwise addition of 50 mM HCl solution. Afterward samples were homogenized (by vortexing and freezing–thawing). The samples were stored for 1 week at 6 °C. The pH of the samples was checked again prior to SAXD measurements. The samples of the $C_{12}NO/DOPE/DNA$ complexes were shortly centrifuged. The precipitate with a few drops of bulk solution was enclosed between two Kapton (Dupont, France) windows of a sample holder for X-ray diffraction.

SANS experiment: the dry $C_{12}NO/DOPE$ mixture was hydrated by 150 mM NaCl in D_2O to get 1 wt% dispersion (pH ~ 7.3). Dispersions were homogenized by vortexing and freezing–thawing, and finally extruded through a polycarbonate membrane filter with 50 nm pores mounted in a mini-extruder (Avestin, Canada). DNA was added at the ratio DNA:lipid = 1:5 base/mol. 40 mM DCl was used to modulate pH of the sample. Samples were measured in 2 mm quartz cells (Hellma, Germany).

2.2. Experimental methods

SAXD experiment: SAXD measurements were performed at the soft condensed matter beamline A2 at HASYLAB at the Deutsches Elektronen Synchrotron (DESY) in Hamburg (Germany), using a monochromatic radiation with a wavelength $\lambda = 0.15$ nm. The scattering pattern was recorded using a 2D Mar CCD detector after tempering the samples at 20 °C. The raw data were calibrated using rat tail collagen [26] and normalized against the incident beam intensity using the purposed-written software A2TOOL. Each diffraction peak of the SAXD region was fitted with a Lorentzian above a linear background. Lattice parameters were determined with uncertainty ± 0.1 Å or less.

SANS experiment: SANS measurements were performed at the small-angle time-of-flight spectrometer YuMO at the IBR-2 fast pulsed reactor of FLNP JINR Dubna (Russia). The necessary requirement for the study of kinetics is an experimental setup allowing mixing two substances in the measuring cell during the process of neutron exposure, or to switch the exposure immediately after mixing. A specific device was required to be used under the conditions of YuMO environment. We constructed such device which allows the injection of the adjusted volume of sample into the measuring cell, under an impulse generated by switching a gas compressor. The switch was terminated out of the experimental hutch. Testing measurements have shown that 3 minutes was a sufficient acquisition time to get a scattering curve of satisfactory quality. To follow the process of structural changes, SANS curves were accumulated in 3 minutes cycles, along a total collecting time equal to ~ 90 minutes. The scattered intensity was normalized by using vanadium standard and corrected for the background effect by the blank sample (150 mM NaCl in D_2O). Temperature was fixed at 20 °C.

3. Results and Discussion

3.1. The structure of $C_{12}NO/DOPE/DNA$

Figure 2A shows the diffractogram of $C_{12}NO/DOPE/DNA$ complexes formed in a solution at neutral pH (~ 7.2). Two peaks ($L(1)$ and $L(2)$) characterize a lamellar phase (L) with repeat distance $d = 54$ Å. Fully hydrated DOPE at 20 °C forms an inverted hexagonal phase with a lattice parameter $a \sim 76$ Å (not shown). The increasing content of $C_{12}NO$ in the mixture induces hexagonal to lamellar phase transition; a lamellar arrangement is observed in all complexes at $C_{12}NO/DOPE > 0.3$ mol/mol [25]. The repeat distance, $d = d_L + d_W$, is the sum of the thicknesses of lipid bilayer, d_L , and of water layer d_W between bilayers. The packing of the L phase is rather poor: the peaks are wide most likely due to small positional order of the elementary cells arrangement, a consequence of lamellae fluctuations.

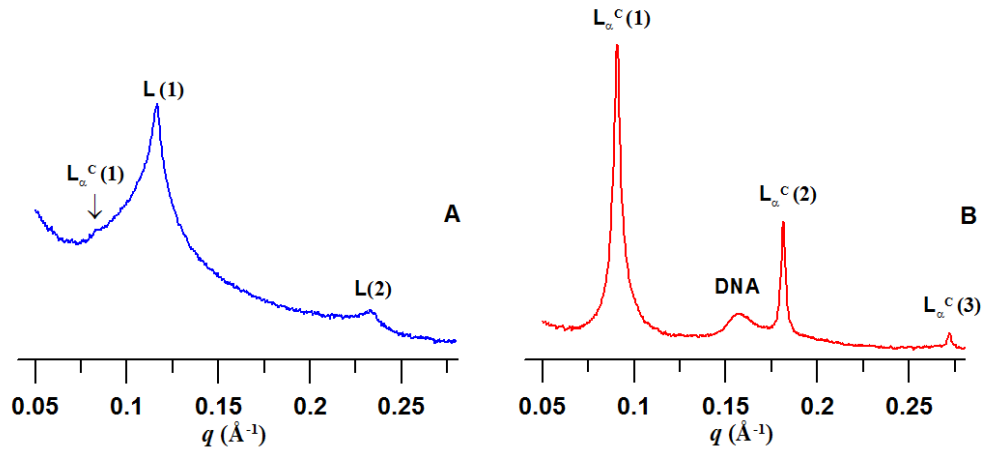


Figure 2. SAXD patterns of $C_{12}NO/DOPE/DNA$ complexes prepared in 150 mM NaCl at pH 7.2 (A) and pH 5 (B).

The DNA uptake is low in neutral solutions. A tiny peak observed at $q \sim 0.084 \text{ \AA}^{-1}$ is detected as the first order peak of a condensed lamellar phase L_{α}^C ($d \sim 75 \text{ \AA}$) with DNA strands packed in water layers between lipid bilayers. We found that a maximum of $\sim 30 \%$ of the total DNA volume in the sample was bound in a condensed lamellar phase L_{α}^C at $C_{12}NO/DOPE=1 \text{ mol/mol}$ and pH 7.2 (see [25] for details). $C_{12}NO/DOPE/DNA$ complexes are sensitive to changes of pH. In acidic solutions, $C_{12}NO$ molecules are protonated, and the surfactant behaves as a cationic agent. The diffractogram of the complex prepared in a solution at pH ~ 5 shows a condensed lamellar phase (Figure 2B). In the acidic solution, the fraction of $C_{12}N^+OH$ is sufficiently high to keep DNA strands arranged regularly between lamellae of L_{α}^C phase, as manifested by the peak related to DNA – DNA packing. Structural parameters of the complexes at selected pH are summarized in Table 1. SAXD experiment confirmed the very good structural responsivity of the complexes to changes of pH.

Table 1. Structural parameters of $C_{12}NO/DOPE/DNA$ complexes

pH	L phase d (\AA)	L_{α}^C phase d (\AA)	d_{DNA} (\AA)
7.2	54.0	75.0	-
6.1	58.2	70.0	42.2
5.0	-	67.7	36.5
4.0	-	64.3	31.4

3.2. Kinetics of $C_{12}NO/DOPE/DNA$ complex formation followed by SANS

In addition to the elastic properties of $C_{12}NO/DOPE$ membrane, electrostatic interactions with DNA polyanion also play an important role in the aggregation process, and thus the complexation geometry is dictated by nontrivial interplay between electrostatic and elastic contributions to the free energy of the complexes [27]. In our system, DNA binding is conditioned by the protonation of molecules of the surfactant. We performed small – angle neutron scattering experiment with the aim to follow kinetics of $C_{12}NO$ protonation and DNA binding.

Figure 3 shows SANS curves of $C_{12}NO/DOPE$ vesicles and a mixture of DNA – $C_{12}NO/DOPE$, at neutral pH. In spite the fact that $C_{12}NO/DOPE$ dispersion was extruded prior to measurements, the curves do not show the typical profile of scattering of unilamellar vesicles like we observed for

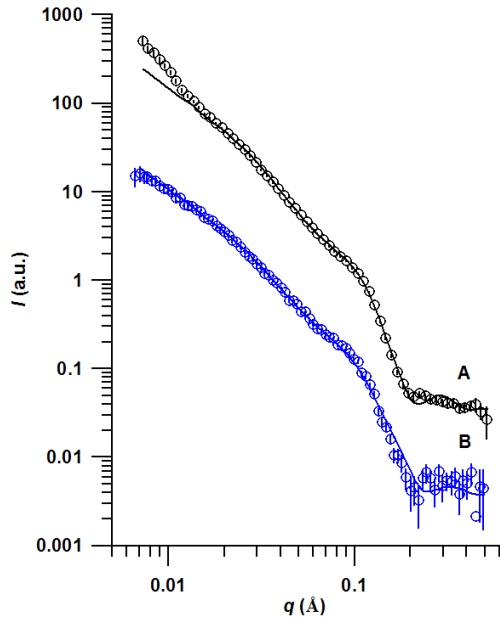


Figure 3. SANS curves of $C_{12}NO/DOPE$ vesicles (A) and a mixture of DNA – $C_{12}NO/DOPE$ (B) in a solution at neutral pH. Full lines show fits using a paracrystal lamellar model.

example in [15]. Due to rapid aggregation, the dispersions are formed by oligolamellar up to multilamellar vesicles.

The SANS data were analyzed using a paracrystal lamellar model with respect to the layer distance distribution and the number of layers in a single cluster [28]. In this model, scattering intensity is given by

$$I(q) = 2\pi(\Delta\rho)^2 \Gamma_m \frac{P_{bil}(q)}{q^2} Z_N(q)$$

where $\Delta\rho$ is the difference in scattering length per unit mass of solute between particles and solvent and Γ_m is the mass per area of the bilayer. The form factor

$$P_{bil}(q) = \left(\frac{\sin(q\xi)}{q\xi} \right)^2$$

where ξ is half the bilayer thickness, and a factor proportional to q^{-2} is typical for an infinitively large two-dimensional sheet. $Z_N(q)$ describes the interference effects for aggregates formed by N layers. Full lines in Figure 3 represent the best fits of experimental data applying this paracrystal lamellar model using SasView fitting software [29]. The average excess of scattering length density per unit mass ($\Delta\rho$) of the solute was calculated from known $C_{12}NO/DOPE$ molar ratio using the appropriate molecular volumes and molecular weights [30, 31]. The ideal model scattering curves were smeared by the instrument resolution $\sim 10\%$. According to the model, the best fit of the scattering curve of $C_{12}NO/DOPE$ (Figure 3A, full line) represents a mixture of uni- and $\sim 30\%$ of oligo-lamellar vesicles consisting of more than 1 bilayer separated with a spacing $\sim 62.6 \text{ \AA}$ with polydispersity of the spacing $\sim 10\%$. We find the lipid bilayer thickness $d_L = 2\xi = 30.3 \pm 0.1 \text{ \AA}$ at the bilayer composition $C_{12}NO/DOPE = 1 \text{ mol/mol}$. To our knowledge, structural data of $C_{12}NO/DOPE$ bilayer are not reported in literature yet. The lipid bilayer consists of a hydrophobic region (d_C) framed by two polar headgroup regions exposed to the water phase. The intercalation of $C_{12}NO$ between DOPE molecules results in a lateral expansion of the interface, and a mismatch between the length of $C_{12}NO$ alkyl substituent and the length of hydrocarbon acyl chains of DOPE (18 carbons) creating defects in the

hydrophobic membrane core. These defects, eliminated by chain bending, lead to a decrease of the thickness (d_C) of the hydrophobic region [14, 32]. In our previous work [15] we found that the thickness of the hydrophobic region of dioleoylphosphatidylcholine (DOPC) bilayer ($d_C=27.4\pm0.1$ Å) decreases to $d_C = 24.9$ Å, and the area per 1 molecule increases from $A = 70.4$ Å² (for DOPC) up to $A = 106.6$ Å² at $C_{12}NO:DOPC=1$ mol/mol. The polar head group of phosphatidylethanolamines is smaller in comparison to that bulky in phosphatidylcholines and also the headgroup region is thinner. For example, at the lipid bilayer thickness $d_L=40.5$ Å of POPE (palmitoyl-oleoylphosphatidylethanolamine) in liquid-crystalline phase (at 35 °C) the thickness of hydrophobic region $d_C = 32.1$ Å was determined by [31], meaning that, the obtained lipid bilayer thickness $d_L = 30.3\pm0.1$ Å for vesicles of $C_{12}NO/DOPE=1$ mol/mol sounds reasonable. At low q values (Figure 3A), we see a clear discrepancy between experimental data and the full line represented by the model. Likely, it is explained by the curvature of vesicles, not taken into account by the model. Figure 3B shows the scattering curve of the $C_{12}NO/DOPE$ dispersion with DNA at pH ~ 7 . The molecules of $C_{12}NO$ are not charged at neutral pH, and thus DNA binding is weak. The full line representing the best fit (using the same model) indicates neither significant change in population of oligolamellar vesicles (~ 30 %) nor in the lipid bilayer thickness. However, due to intercalation of DNA polyanion between bilayers without efficient screening of its negative charges, the repeat distance increases to ~ 78 Å with polydispersity ~ 20 %. The obtained repeat distance is close to ~ 75 Å detected by SAXD in L_α^C phase at similar conditions.

We injected adjusted volume of diluted DCl in the measuring cell containing a mixture of DNA and $C_{12}NO/DOPE$ vesicles (pH 7) with the aim to follow kinetics of DNA binding due to protonation of $C_{12}NO$ molecules. SANS data were collected in 3 min cycles. Dependences of SANS intensity $I(q)$ on scattering vector q for DNA – $C_{12}NO/DOPE$ dispersion along the measuring time are depicted in Figure 4. The initial q dependence (red circles) shows the scattering of DNA – $C_{12}NO/DOPE$ dispersion at pH ~ 7 , prior to DCl injection. In a solution at neutral pH, the interaction between DNA and $C_{12}NO/DOPE$ vesicles is weak, and we observed uni – or oligolamellar structures, as discussed above. The injected DCl changes pH in the measuring cell from 7 to 4. The interaction of DNA with $C_{12}NO/DOPE$ vesicles under acidic conditions results in the disintegration of vesicles and the formation of multilamellar structures, similarly to DNA - cationic liposome complexes. All curves were fitted by the same paracrystal lamellar model using SasView software. Excellent accord is obtained. An example of the distribution of residuals is shown in Figure 4, inset. The system was followed along 90 minutes. Figures 5A - C show the time evolution of the obtained structural parameters: the number of layers (Figure 5A), the lipid bilayer thickness (Figure 5B) and the spacing (Figure 5C). Our experiment indicates that both processes the protonation of $C_{12}NO$ molecules and DNA binding are rapid. We detected substantial growth of clusters due to DNA complexation reaching up to ~ 32 layers already in three minutes after the DCl injection (Figure 5A). Beyond this rapid aggregation, we detected further growth of aggregates. The number of layers increases gradually, and about ~ 4 additional layers were attached during the followed time interval. Cryoelectron microscopy observations [33] report that most likely the DNA – cationic liposomes complex growth begins with one DNA – coated vesicle. In this way DNA acts as a molecular “glue” enforcing close apposition of neighbour vesicle. Multilamellar lipid – DNA complexes appear to form by mechanism that involves the rupture of an approaching vesicle and subsequent adsorption of its membrane to a “template” vesicle or a lipid-DNA complex. The authors [33] do not exclude also another mechanism, when the attached vesicle is flattened, and is adsorbed to a “template” vesicle. However, in this way, the complex grows always with even number of layers. In such mechanism one can not exclude alternation of layers consisting of the lipid only, and those with DNA. The complexes frequently exhibit partially open bilayer segments on their outside surfaces. DNA accumulates near the edges of such unusually terminated membranes. The full line in Figure 5A shows the fit of experimental points by a Boltzmann function indicating the growth of complexes by cooperative process. Our experiment shows that DNA complexation is rapid and the “ground” of complexes was formed in time domain before three minutes after the acidification. The observed growth can be interpreted as an adsorption

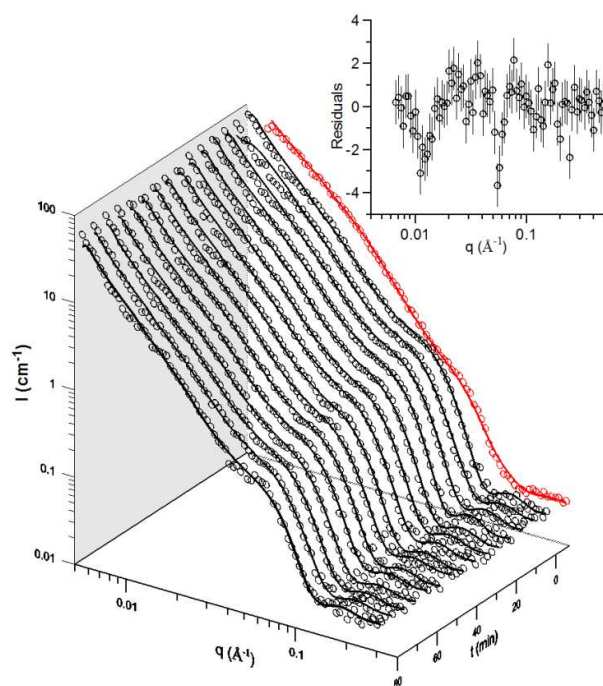


Figure 4. Dependences of SANS intensity $I(q)$ on scattering vector q for DNA – C₁₂NO/DOPE dispersion as a function of time; prior (red points) and after DCI injection. Full lines show fits using a paracrystal lamellar model.

Inset: An example of the distribution of residuals.

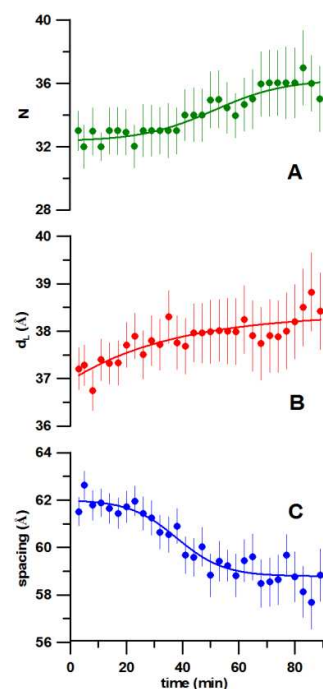


Figure 5. Time dependence of the structural parameters: the number of layers (A), the lipid bilayer thickness (B) and the spacing (C).

of further oligo-lamellar vesicles to the complex at any of its rims (with DNA accumulated) that might exist.

Figure 5B shows changes in the lipid bilayer thickness. Both C₁₂NO protonation and structural changes in the polar region of the bilayer due to DNA binding result in the increase of the lipid bilayer thickness up to $d_L \sim 37$ Å, in three minutes after the DCI injection. Next, a slight increase in d_L (~ 1 Å) manifests internal re-organization of the complexes. Modelling [34, 35] and experimental studies [36] confirms a direct involvement of the neutral lipids in the electrostatic interaction with DNA. Due to the cationic additive, the P⁻-N⁺ dipole of the phospholipid headgroup changes its orientation [37], exposing the N⁺ end towards the aqueous environment and interacts with the complexed DNA. Accordingly, DNA can induce additional changes of the orientation of P⁻-N⁺ dipole due to Coulombic attraction. This results in a reduction average area occupied by PE headgroup. Reorientation of P⁻-N⁺ dipole, and H⁺ (or D⁺) binding due to the C₁₂NO protonation can yield electrostatic interactions at the headgroup level. As a consequence, chain-chain interactions within the hydrophobic core increases balancing forces in the membrane lateral pressure profile. We suppose that these molecular changes are responsible for the lipid bilayer increase, as shown in Figure 5B.

Figure 5C shows time evolution of the spacing. Both experiments (SAXD and SANS) confirm a weak binding of DNA between the lamellae of the C₁₂NO/DOPE vesicles at neutral pH. After DCI injection, H⁺ (D⁺) diffusion can be considered as the driving force of aggregation. C₁₂NO⁺H molecules act as a cationic surfactant. The drop of the spacing from ~ 78 Å to ~ 62 Å in three minutes proves the efficient screening of negative charges of DNA condensed between the lipid bilayer. It is worth mentioning that the model for data treatment includes polydispersity of the spacing, which is ~ 43 %.

The resolution of SANS instrument is lower in comparison to SAXD. Indeed, SANS curves (Figure 4) show a broad peak at $q \sim 0.1 \text{ \AA}^{-1}$ smeared because of instrumental resolution. The obtained value, $\sim 62 \text{ \AA}$, is in good accord with the repeat distance $d = 64.3 \text{ \AA}$ of a condensed lamellar phase of $C_{12}\text{NO}/\text{DOPE}/\text{DNA}$ complexes at pH 4 derived from SAXD (Table 1). The thickness of $C_{12}\text{NO}/\text{DOPE}$ bilayer forming the complexes is $d_L \sim 37\text{--}38 \text{ \AA}$ (Figure 5B). Thus the water gap of thickness $d - d_L \sim 25 \text{ \AA}$ fits exactly for an intake of hydrated DNA strands with a diameter $\sim 25 \text{ \AA}$ [38]. The contrast between DNA and buffer is small at the used DNA concentration and thus its contribution to the SANS scattering intensity is negligible. Figure 5C shows a marked drop in the spacing, from $\sim 62 \text{ \AA}$ to $\sim 59 \text{ \AA}$, proving an evolution of the system during the time followed by SANS experiments. In spite of high polydispersity ($\sim 43 \%$), to accommodate DNA with a diameter $\sim 25 \text{ \AA}$ into a lamellar phase with spacing $\sim 59 \text{ \AA}$ would suppose thinning of the lipid bilayer. As mentioned above, one of mechanisms of the complexes growth supposes an adsorption of flattened vesicles to a “template” vesicle [33]. In this way, the complex grows always with even number of layers. Moreover bilayers that include DNA can alternate with bilayers without DNA. Such structures are frequently formed at DNA aggregation with neutral phosphatidylcholines in presence of divalent cations, and were detected by SAXD [39 - 41]. The coexistence of two lamellar phases within one structure was observed also for $C_{12}\text{NO}/\text{DOPE}/\text{DNA}$ complexes at pH > 6 (see Table 1) [25]. A careful inspection of structural data tells, that the repeat distance of L_α^C phase decreases with pH, while L phase swells due to excess of non-compensated positively charged $C_{12}\text{NO}^+\text{H}$ molecules. Note that, at acidic conditions the repeat distances of both phases are close, and likely can-not be resolved by SANS technique. In respect to high polydispersity of the spacing, we suppose that DNA is condensed in each of both structures; however bilayers depleted of DNA are slightly prevailing in clusters with smaller spacing ($\sim 59 \text{ \AA}$). The observed drop of the spacing can be attributed to internal reorganization, and likely related to redistribution of DNA, actually its release. Lipoplexes show best stability at the isoelectric point, when the numbers of positive and negative charges are equal [27]. The overcharging of the complex away from its isoelectric point is caused by changes of the bulk structure with absorption of excess DNA or cationic lipid. Importantly, overcharged complexes are observed to move toward their isoelectric charge-neutral point at higher concentration of salt co-ions, with positively overcharged complexes expelling cationic lipid and negatively overcharged complexes expelling DNA [42]. Moreover, high ionic strength reduces the fraction of bound DNA in the complexes, and the isoelectric point is attained at lower ratio DNA/cationic additive than the one that can be estimated by calculations based on their nominal charges [43]. Our lipoplexes were formed in aqueous medium at high ionic strength (150 mM NaCl). The fit of experimental points in Figure 5C by Boltzmann function shows $t = 38.0 \pm 2.9 \text{ min}$ as inflection point for DNA release. However, the sigmoid in Figure 5A, related to the growth of complexes, shows the inflection point later, at $t = 51.3 \pm 4.9 \text{ min}$. This time succession offers an explanation why DNA released from the complexes can mediate the adsorption of the next approaching vesicle and form additional layers in this lamellar structure.

4. Conclusion

We used N,N-dimethyldodecylamine-N-oxide ($C_{12}\text{NO}$) for designing of a pH sensitive DNA delivery vector. SAXD experiments show the necessary structural responsivity of $C_{12}\text{NO}/\text{DOPE}/\text{DNA}$ complexes to changes of pH in aqueous medium at high ionic strength. SANS data in kinetic experiments were analysed using a paracrystal lamellar model in order to follow time evolution of the complexes, their growth, changes in the lipid bilayer thickness and spacing. The protonation of the surfactant molecules in $C_{12}\text{NO}/\text{DOPE}$ mixture is rapid, and multilamellar $C_{12}\text{NO}/\text{DOPE}/\text{DNA}$ complexes with ~ 32 layers are formed before 3 minutes. In the time domain above 3 minutes, there is further reorganization of the complexes likely due to moving the structure towards its higher stability at isoelectric point.

Our experiments confirm that N,N-dimethylalkylamine-N-oxides show excellent pH responsivity changing their property from nonionic to cationic in a narrow window of pH. This ability is preserved also when molecules of the surfactant are mixed with a neutral phospholipid, what suggests their

utilization for designing genetic material delivery vectors, also for nanocarriers on targeted drug delivery.

Acknowledgements

The authors thank S. S. Funari for his assistance on SAXD measurements. This work benefitted from SasView software, originally developed by the DANSE project under NSF award DMR-0520547. The research has received funding from the European Community's Seventh Framework Programme (FP7/2007-2013) under grant agreement n° 226716 (HASYLAB project II-20100372 EC); JINR project 04-4-1121-2015/2017 and grant VEGA 1/0916/16.

References

- [1] Felgner P L, Gadek T R, Holm M, Roman R, Chan H W, Wenz M, Northrop J P, Ringold G M and Danielsen M 1987 *Proc. Natl. Acad. Sci. U. S. A* **84** 7413
- [2] Lasic D D and Templeton N S 1996 *Adv. Drug Deliv. Rev.* **20** 221
- [3] Fattal E, Couvreur P and Dubernet C 2004 *Adv. Drug Deliv. Rev.* **56** 931
- [4] Sakaguchi N, Kojima C, Harada A, Koiwai K and Kono K 2008 *Biomaterials* **29** 4029
- [5] Ganta S, Devalapally H, Shahiwala A and Amiji M 2008 *J. Control. Release* **126** 187
- [6] Simoes S, Moreira J N, Fonseca C, Duzgunes N and de Lima M C P 2004 *Adv. Drug Deliv. Rev.* **56** 947-65
- [7] Maeda H, Tsunoda M and Ikeda S 1974 *J. Phys. Chem.* **78** 1540
- [8] Búcsi A, Karlovská J, Chovan M, Devínsky F and Uhríková D 2014 *Chem. Pap.* **68** 842
- [9] Singh S K, Bajpai M and Tyagi V K 2006 *J. Oleo Sci.* **55** 99
- [10] Devínsky F 1985 *Acta Fac. Pharm. Univ. Comen.* **40** 63
- [11] Šeršeň F, Leitmanová A, Devínsky F, Lacko I and Balgavý P 1989 *Gen. Physiol. Biophys.* **8** 133
- [12] Dubničková M, Kiselev M, Kutuzov S, Devínsky F, Gordeliy V and Balgavý P 1997 *Gen. Physiol. Biophys.* **16** 175
- [13] Barlow D J, Lawrence M J, Zuberi T, Zuberi S and Heenen R K 2000 *Langmuir* **16** 10398
- [14] Karlovská J, Degovics G, Lohner K, Lacko I, Devínsky F and Balgavý P 2004 *Chem. Phys. Lipids* **129** 31
- [15] Belička M, Kučerka N, Uhríková D, Islamov A Kh, Kuklin A, Devínsky F and Balgavý P 2014 *Eur. Biophys. J.* **43** 179
- [16] Uhríková D, Kučerka N, Islamov A, Gordeliy V and Balgavý P 2001 *Gen. Physiol. Biophys.* **20** 183
- [17] Devínsky F, Kopecká-Leitmanová A, Šeršeň F and Balgavý P 1990 *J. Pharm. Pharmacol.* **42** 790
- [18] Bukovský M, Mlynářčík D and Ondráčková V 1996 *Int. J. Immunopharmacol.* **18** 423
- [19] Warisnoicharoen W, Lansley A B and Lawrence M J 2003 *J. Pharm. Sci.* **92** 859
- [20] Mel'nikova Y S and Lindman B 2000 *Langmuir* **16** 5871
- [21] Wang Y, Dubin P L and Zhang H 2001 *Langmuir* **17** 1670
- [22] Bonincontro A, Marchetti S, Onori G and Santucci A 2003 *Chem. Phys. Lett.* **370** 387
- [23] Goracci L, Germani R, Savelli G and Bassani D M 2005 *Chembiochem* **6** 197
- [24] Marchetti S, Onori G and Cametti C 2005 *J. Phys. Chem. B* **109** 3676
- [25] Hubčík L, Funari S S, Pullmannová P, Devínsky F and Uhríková D 2015 *Biochim. Biophys. Acta* **1848** 1127
- [26] Roveri N, Bigi A, Castellani P P, Foresti E, Marchini M and Strocchi R 1980 *Boll. Soc. Ital. Biol. Sper.* **56** 953
- [27] May S, Harries D and Ben Shaul A 2000 *Biophys. J.* **78** 1681
- [28] Bergstrom M, Pedersen J S, Schurtenberger P and Egelhaaf S U 1999 *J. Phys. Chem. B* **103** 9888
- [29] SasView, <http://www.sasview.org/>
- [30] Belička M, Klacsová M, Karlovská J, Westh P, Devínsky F and Balgavý P 2014 *Chem. Phys. Lipids* **180** 1

- [31] Kučerka N, van Oosten B, Pan J, Heberle F A, Harroun T A and Katsaras J 2015 *J. Phys. Chem. B* **119** 1947
- [32] Balgavý P and Devínsky F 1996 *Adv. Colloid Interface Sci.* **66** 23
- [33] Huebner S, Battersby B J, Grimm R and Cevc G 1999 *Biophys. J.* **76** 3158
- [34] Bandyopadhyay S, Tarek M and Klein M L 1999 *J. Phys. Chem. B* **103** 10075
- [35] Pink D A, Quinn B, Moeller J and Merkel R 2000 *Phys.Chem.Chem. Phys.* **2** 4529
- [36] Ryhanen S J, Saily MJ , Paukku T, Borocci S, Mancini G, Holopainen J M and Kinnunen P K J 2003 *Biophys. J.* **84** 578
- [37] Scherer P G and Seelig J 1989 *Biochemistry* **28** 7720
- [38] Radler J O, Koltover I, Salditt T and Safinya C R 1997 *Science* **275** 810
- [39] McManus J, Radler J O and Dawson K A 2003 *Langmuir* **19** 9630
- [40] Francescangeli O, Stanic V, Gobbi L, Bruni P, Iacussi M, Tosi G and Bernstorff S 2003 *Phys. Rev. E* **67** 011904
- [41] Uhríková D, Hanulová M, Funari S S, Khusainova RS, Šeršeň F and Balgavý P 2005 *Biochim. Biophys. Acta* **1713** 15
- [42] Koltover I, Salditt T and Safinya C R 1999 *Biophys. J.* **77** 915
- [43] Pullmannová P, Bastos M, Guangyue B, Funari SS, Teixeira J, Lacko I and Uhríková D 2012 *Biophys. Chem.* **160** 35